Extended Abstracts of the 2020 International Conference on Solid State Devices and Materials, VIRTUAL conference, 2020, pp219-220

D-4-06 (Late News)

Development of Analytical Channel Mobility Model Based on Study of Universal Mobility in SiC MOSFET

Teruyuki Ohashi[1], Ryosuke Iijima[1] and Hiroshi Yano[2]

[1]Corporate Research & Development Center, Toshiba Corporation, Kawasaki, Kanagawa 212-8582, Japan
Phone: +81-44-549-2142 E-mail: teruyuki.ohashi@toshiba.co.jp
[2]Graduate School of Pure and Applied Sciences, University of Tsukuba, Tsukuba, Ibaraki 305-8573, Japan

Abstract

An analytical channel mobility model of SiC MOSFET has been constructed based on the results of experimental and theoretical investigation of the universal mobility. Experimental results including temperature dependence have been well reproduced by this model.

1. Introduction

The performance of SiC MOSFET is limited by the low channel mobility. Figure 1 shows general mechanisms limiting the channel mobility. To further improve the mobility, a systematic understanding of the scattering mechanism is essential. Figure 2 shows a comparison of the effective channel mobility (μ_{eff}) of conventional SiC MOSFETs [1] with the universal mobility of Si MOSFETs [2]. In Si MOSFETs, μ_{eff} shows a universal curve when expressed as a function of effective electric fields (E_{eff}) regardless of acceptor concentration (N_{A}), substrate bias (V_{b}), and nominal process conditions. This universal curve is called universal mobility and is understood in association with the scattering mechanism. Therefore, from the comparison of μ_{eff} in fabricated MOSFETs with the universal mobility, the dominant scattering mechanism can be estimated. In addition, the analytical model of universal mobility is built and utilized in device and circuit simulation. However, universal mobility cannot be obtained in conventional SiC MOSFETs as shown in Fig. 2.

Figure 3 shows our approach for achieving a systematic understanding of the scattering mechanism in SiC MOSFETs. In our previous study, we obtained the universal mobility of SiC MOSFETs experimentally [3]. This universal mobility was compared with theoretical calculation results, and the mobility limited by each scattering mechanism was extracted [4]. In this study, these results are discussed comprehensively and an analytical model based on these experimental and theoretical results is presented.

2. Results and discussion

Figure 4 shows the experimentally obtained μ_{eff} of SiC MOSFETs [3]. Defects at MOS interfaces were reduced by wet oxidation on C-face substrates. In addition, electron trapping to wet oxide was suppressed by pulse measurement, and then the universal mobility of SiC MOSFETs was obtained.

Then, the theoretical calculation of the channel mobility was performed based on [5-6]. Figure 5 shows calculated results of acoustic phonon scattering limited mobility (μ_{ac}). In 4H-SiC substrates, there are two proximity conduction band minima (CBM) at the *M* point in the Brillouin zone. It can be seen that μ_{ac} is decreased due to interband scattering at high E_{eff}. As shown in Figs. 6(a) and 6(b), the energy and occupation ratio difference of the two CBM decreases with E_{eff}. Therefore, the higher the E_{eff}, the higher the scattering rate between the two CBM, leading to the decrease in μ_{ac}. Similarly, mobility limited by surface roughness scattering (μ_{sr}) and mobility limited by intervalley scattering due to optical phonon (μ_{inter}) were calculated [4]. The total mobility was obtained from Matthiessen's rule and compared to experimental results as shown in Fig. 7(a). Using parameters listed in Fig. 7, experimental results were well reproduced. Figure 7(b) shows separately plotted μ_{ac}, μ_{inter} and μ_{sr}. It can be seen that μ_{ac} is dominant in a wide E_{eff} range and the influence of μ_{sr} increases at high E_{eff}.

Based on these experimental and calculation results, we tried to construct an analytical model. Equations (1) – (3) in Fig. 8(a) show analytical formulas. μ_{ac} and μ_{inter} are expressed together as μ_{ph}, and μ_{ph} and μ_{sr} are combined by Matthiessen's rule to obtain μ_{tot}. Figure 8(b) shows fitting results of the E_{eff}'s exponents α_{ph} and α_{sr} for μ_{ph} and μ_{sr}. In previous works [3,7], α_{ph} was set to a constant value regardless of the E_{eff} range, as well as Si MOSFETs. However, due to the influence of scattering between two CBM, α_{ph} decreased linearly with E_{eff}. Figure 9(a) and 9(b) show the temperature dependence of the mobility in the medium and high E_{eff} regions, respectively. In the medium E_{eff} region, where the influence of phonon scattering is strong, μ_{eff} was proportional to $T^{-0.65}$, which is close to μ_{ac} of Si MOSFETs. In the high E_{eff} region, the temperature dependence became smaller, which is considered to be due to the greater influence of roughness scattering. These trends are consistent with the results in Fig. 7(b). Figure 10 shows the comparison of theoretical and analytical calculation results. It can be seen that the analytical model well reproduces theoretical calculation results. Figure 11 shows analytical calculation results of the temperature dependence of μ_{eff}. It can be seen that experimental results are well reproduced by the analytical model.

3. Conclusions

Based on experimental and theoretical findings concerning the universal mobility, an analytical model was constructed. Unlike in previous studies, the E_{eff}'s exponent α_{ph} for μ_{ph} (when μ_{ph} is expressed as $\mu_{\mathrm{ph}} = kE_{\mathrm{eff}}^{\alpha_{\mathrm{ph}}}$) decreased linearly with E_{eff} due to the acoustic phonon scattering between the two CBM. This model is semi-physical and well reproduces experimental results including temperature dependence, and will be useful in device and circuit simulation.

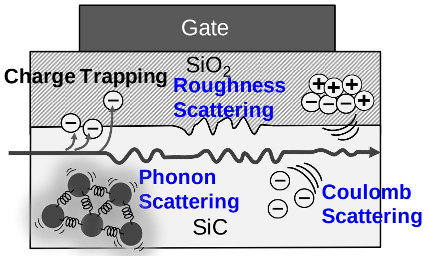

Fig. 1 Schematic diagram of scattering mechanisms and charge trapping to interface states and bulk SiO_2 in SiC MOSFETs.

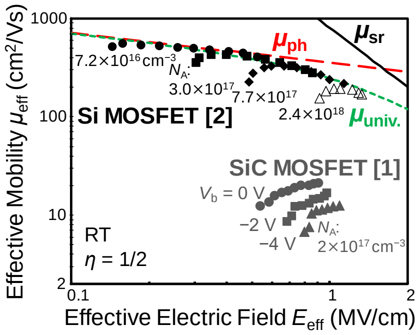

Fig. 2 Comparison of universal mobility in Si MOSFETs [2] with mobility in conventional SiC MOSFETs [1].

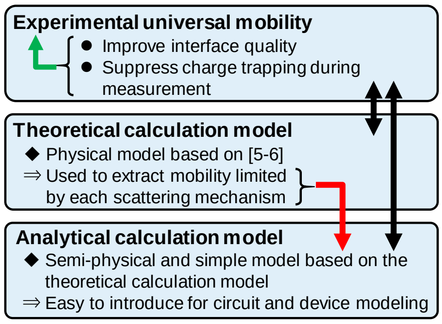

Fig. 3 Our approach for achieving a deeper understanding of the scattering mechanism of SiC MOSFET.

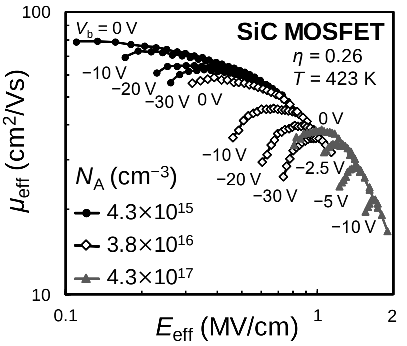

Fig. 4 Universal mobility of SiC MOSFET obtained experimentally in our previous study [3].

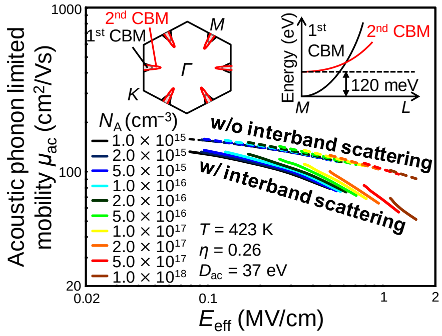

Fig. 5 Theoretical calculation results of acoustic phonon limited mobility (μ_{ac}). μ_{ac} is degraded by scattering between two proximity conduction band minima (CBM).

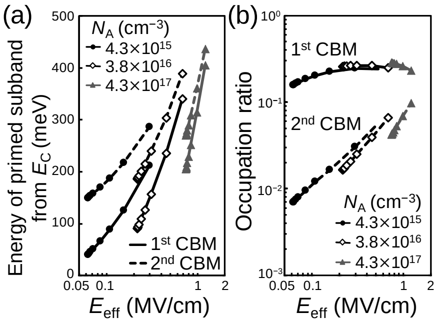

Fig. 6 (a) Energy of primed subband and (b) occupation ratio. At high E_{eff}, energy and occupation ratios of the two bands approach and interband scattering rate increases.

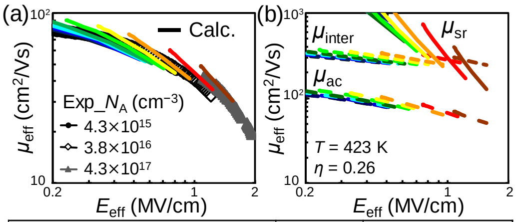

	Symbol	Value
Deformation potential for μ_{ac}	D_{ac}	37 eV
Deformation potential for μ_{inter}	d_{inter}	1.2×10^{11} eVm^{-1}
Optical phonon energy for μ_{inter}	$\hbar\omega_{inter}$	0.085 eV
Height of roughness	Δ	5.7×10^{-10} m
Correlation length of roughness	Λ	1.7×10^{-9} m

Fig. 7 (a) Comparison of theoretically calculated mobility with the experimental data. (b) Separately plotted μ_{ac}, μ_{inter} and μ_{sr}. Table shows parameters used in calculation.

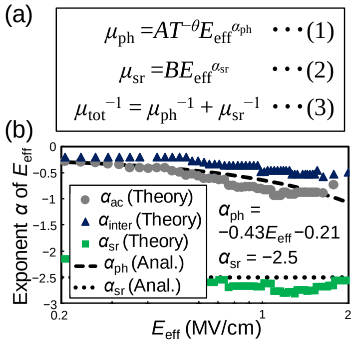

Fig. 8 (a) Simple analytical mobility model constructed in this study. (b) Experimental and fitting results of E_{eff}'s exponents α_{ph} and α_{sr}.

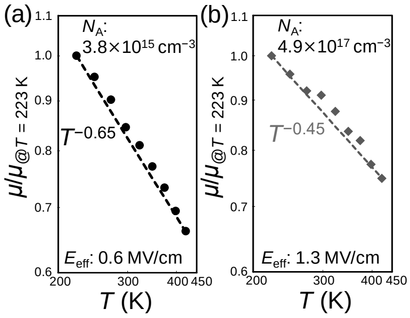

Fig. 9 Temperature dependence of mobility at (a) $E_{eff} = 0.6$ MV/cm and (b) $E_{eff} = 1.3$ MV/cm. Dashed lines show fitting.

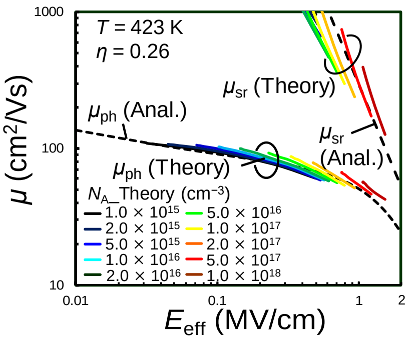

Fig. 10 Comparison of theoretical calculation and analytical calculation. μ_{ph} and μ_{sr} were reproduced separately.

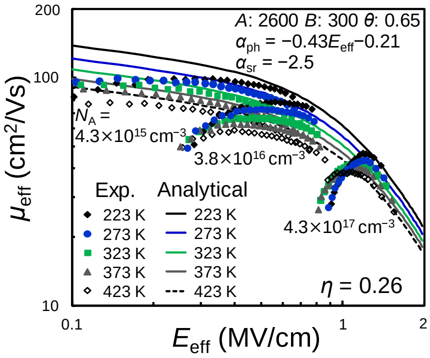

Fig. 11 Calculation of temperature dependence of μ_{eff}–E_{eff} curve by analytical model. Experimental result is well reproduced by analytical model.

References

[1] V. Tilak *et al.*, IEEE Trans. Electron Devices **54**, 2823 (2007).

[2] S. Takagi *et al.*, IEEE Trans. Electron Devices **41**, 2357 (1994).

[3] T. Ohashi *et al.*, IEEE Trans. Electron Devices **65**, 2707 (2018).

[4] T. Ohashi *et al.*, Jpn. J. Appl. Phys. **59**, 034003 (2020).

[5] K. Masaki *et al.*, Jpn. J. Appl. Phys. **28**, 1856 (1989).

[6] H. Iwata *et al.*, J. Appl. Phys. **88**, 1956 (2000).

[7] M. Noguchi *et al.*, IEDM Tech. Dig., 2017, p. 219.